

PARTIAL MELTING MECHANISM AND MANTLE PERIDOTITE CHEMICAL GEODYNAMICS

M. LOUBET and U. A. LAR

(Received 19 July 1999; Revision accepted 6 December, 1999)

ABSTRACT

Peridotite samples collected during ODP Leg 109 drilling on the flanks of the Mid-Atlantic Ridge (MAR) (23° 10'N) were analysed for major, trace elements and isotopic compositions. As is common of abyssal peridotite, the samples have been affected by variable degrees of serpentinization. The data is in favour of the residual nature of these mantle peridotites, with compositional characteristics intermediate between slightly depleted orogenic harzburgites and highly depleted ophiolitic harzburgites. The modeling of the conditions of partial melting of these peridotites, based on analysis of the Nd to Lu part of the REE spectra (which appears to be unaffected by the serpentinization process), supports partial melting processes operating at equilibrium at least during specific stages of the process, with moderate degrees of partial melting (9% to 14%). The degree of equilibrium attained between segregating melts and residues is sensitive to the ascent rate of the mantle diapirs. Some evaluations have shown that equilibrium can operate when spreading rates and inferred ascent of mantle diapirs are small as is the case at 23° on the M.A.R. The equilibrium/disequilibrium type of melting might represent another characteristic distinguishing mantle peridotites coming from different geodynamic environments (Lherzolite orogenic massifs, Harzburgite Ophiolite massif, this Leg 109 Mid oceanic ridge section), which is indicative of their different conditions of melting.

Keywords: mantle peridotite, mantle diapir, partial melting, modeling.

INTRODUCTION

Peridotites recovered from, Hole 670 A during the Ocean Drilling Project (Leg 109) on the flanks of the MAR (23° 10'N) consist of a sequence of harzburgites affected by variable degrees of serpentinization (Shipboard Scientific Party, 1988, Site 670).

Occurrences of peridotite outcrops are variably distributed beneath all oceans. However, most of these outcrops are exposed along large fracture zones associated with transform faults or away from the axial rift valley in relatively recent oceanic crust or from trenches at the margin of ocean basins (Bonatti and Hamlyn, 1981; Dick et al; 1984). In the Atlantic ocean they appear to occur rather frequently (Bonatti and Hamlyn, 1981; Michael and Bonatti 1985a, b, Juteau et al., 1990) and various reasons for this wide occurrence of peridotite outcrops in the Atlantic have been advanced (Karson et al., 1987; Dicket al., 1984; Juteau et al; 1990).

Mantle peridotites vary in composition from lherzolitic (in alpine or

orogenic bodies) to harzburgitic (in ophiolite bodies) (Nicolas and Jackson, 1972; Boudier and Nicolas, 1986). These two types of peridotite are distinguished by their significantly different rare earth element (REE) patterns. The first group exhibit slightly depleted light REE patterns whereas the second group exhibit heavy REE contents of about 2x chondritic abundances and highly impoverished REE concentrations with a significant light REE enrichment (Loubet et al., 1975; Frey, 1982, Ottonello, 1980; Ottonello et al., 1984 a,b; Pallister and Knight, 1981, Frey et al, 1985, Menzies, 1984.). These peridotites are residual, resulting from a variable degree of partial melting (from low for the orogenic lherzolites to high for the harzburgitic ophiolites

Ocean floor or Abyssal peridotites display compositions that extends well over the range of mantle peridotites. They normally display slightly to moderately depleted compositions, and do not attain the high depletion of the ophiolite harzburgites (Dick and Bullen, 1984; Michael and Bonatti, 1985b). The Leg 109

Preliminary Report (Shipboard Scientific Party, 1988) suggest that these M.A.R. peridotites could be residual, and apparently display intermediate to relatively depleted compositions. If these rocks are residual, they will provide information on : 1. the structure and composition of the oceanic mantle below the Mid-Atlantic Ridge and possibly on the genetic relationships between the ridge basalt and the peridotitic mantle. 2. the fusion processes which affected these segments "en route" to the surface. The fusion processes within the mantle with respect to the origin and nature of the magmas formed, whether in equilibrium or not (Prinzoffer and Allegre, 1985); and the way the magmas are extracted and transported to the surface (McKenzie; 1984, Spera, 1980; Nicolas, 1986) has given rise to several proposals. These residual rocks are of paramount importance for the analysis of the fusion processes because they may enable a direct identification of the primary magmas. This task is extremely difficult with magmas found at the surface because the emitted magmas largely represent, an accumulation of numerous patches of primary magmas which suffered fractional crystallization before their eruption.

This paper is not only intended to present the geochemistry of Leg 109 peridotites but also to, on the basis of REE distribution of these rocks discuss the conditions of their fusion and the plausibility of the equilibrium and disequilibrium types of fusion to occur in mantle diapirs rising at oceanic ridges and in different mantle

TABLE 1 Major element contents of 23° 10' N MAR Leg 109 peridotites

Leg 109

	P5-2-9 73 - 75	P5 - 2 - 13 100 - 103	P5 - 2 - 15 116 - 118	P6 - 1-3 16 - 19
SiO ₂	36.79	36.77	36.96	37.60
TiO ₂	0.03	0.03	0.03	0.03
Al ₂ O ₃	1.56	1.36	1.64	1.76
Fe ₂ O ₃ *	8.23	8.47	7.94	8.12
MnO	0.10	0.08	0.08	0.08
MgO	39.43	39.95	39.34	39.40
P ₂ O ₅	0.03	0.02	0.02	0.02
CaO	1.62	1.12	0.89	1.20
K ₂ O	0.02	0.01	0.02	0.09
Na ₂ O	0.13	0.19	0.15	0.17
H ₂ O	12.93	13.32	13.52	12.62
Total	100.87	101.32	100.59	101.09

*Total Fe as Fe₂O₃

geodynamic environments.

ANALYTICAL TECHNIQUES

The major elements, (except for Na and K), were measured by X-Ray Fluorescence (XRF) on a Siemens X-ray Spectrometer in the Toulouse University Petrological laboratory using fused pellets with the classical heavy absorber method. Na and K were analysed by flame spectrometry at the Geochemical Laboratory of Toulouse University (GLTU). Volatile elements were determined by loss on ignition at 1000°C. Analytical accuracy (and precision) is considered to be better than 2%

XRF spectrometry using pressed powder pellets (with a 10% weight binder) was used to analyze certain trace elements (Ti, V, Cr, Co, Ni, Nb, Zr). Matrix, instrumentation as well as interference and enhancement effects were corrected by computation with methods developed by Bougault et al., (1977). Selected international rock standards (Nancy CRPG standards) were used for calibration. Analytical accuracy for trace elements other than Nb was within 5% to 10% for concentrations higher than 20 ppm. This accuracy was ±2 ppm at lower concentrations.

REE, Rb, Sr, and Ba concentrations were measured by isotope dilution at the GLTU on a modified CAMECA THN 206 MASS SPECTROMETER. Accuracy for these analyses was estimated at approximately 2%. Chemical separation of the elements was carried out on a AG 50 W (200-400 mesh) cationic ion exchange column. Sr was separated from Ca using

RESULTS

The major and trace elements data (including the REE) are reported on Tables 1 and 2.

Major /Trace element composition

The peridotite analysed exhibit compositions that compare with the fields of compositions of mantle peridotites from different geodynamic environments such as peridotites from orogenic massifs (Frey et al., 1985, Bonatti et al., 1986), and highly depleted ophiolitic harzburgites (Dick and Bullen, 1984).

Similarly, they also display trace element compositions (Ni, Co, Cr, Y, and Yb) that compare with the typical composition range of mantle peridotites. In the (Ni, MgO) diagram of Fig.2a and in the (CaO, Yb) diagram of Fig.2b, the Leg 109 peridotites

XRF: X-Ray Fluorescence
ID: Isotope dilution

TABLE 2: Trace element contents of 23° 10'N MAR Leg 109 peridotites

Table	V XRF	V ID	Cr XRF	Co XRF	Ni XRF	Zn XRF	Ba ID	Ba XRF	Rb ID	Rb XRF	Sr XRF	Sr ID	Nd XRF	Nd ID	Zr XRF	Sm ID	Eu ID	Gd ID	Dy ID	Y XRF	Y ID	Yb ID	Lu ID
P5-1-6	156	59	2362	123	2369	46	0.064	0	0.01	0.830	0.00	0.92	0.018	0.015	12	0.012	0.008	0.033	0.060	4.200	0.060	0.060	0.011
P5-2-9	156	51	1893	135	2489	37	2.980	0	0.02	5.390	0.03	1.11	0.015	7	0.010	0.010	0.040	0.073	4.200	0.068	0.068	0.013	
P5-2-13	156	62	2350	120	2275	35	4.000	0	0.01	1.260	2.28	1.34	0.019	11	0.010	0.005	0.029	0.090	2.600	0.074	0.074	0.014	
P5-2-15	156	64	2721	120	2329	51	0.021	0	0.005	2.340	0.77	1.09	0.017	112	0.011	0.006	0.033	0.064	2.500	0.077	0.077	0.015	
P6-1-3							0.014	0.022	0.007	0.007	0.007	1.76	0.025	0.016	0.016	0.009	0.038	0.071	0.070	0.065	0.065	0.012	
P6-1-5(a)							0.051	0.095	0.007	0.007	0.007	0.008	0.008	0.008	0.0036	0.001	0.001	0.0076	0.0182	0.0442	0.0442	0.013	
P9-1-2(a)							0.007	0.0189				0.014	0.014	0.014	0.0082	0.005	0.005	0.0363	0.0470	0.0530	0.0530		
P9-1-2(b)																							
P6-1-5(b)																							

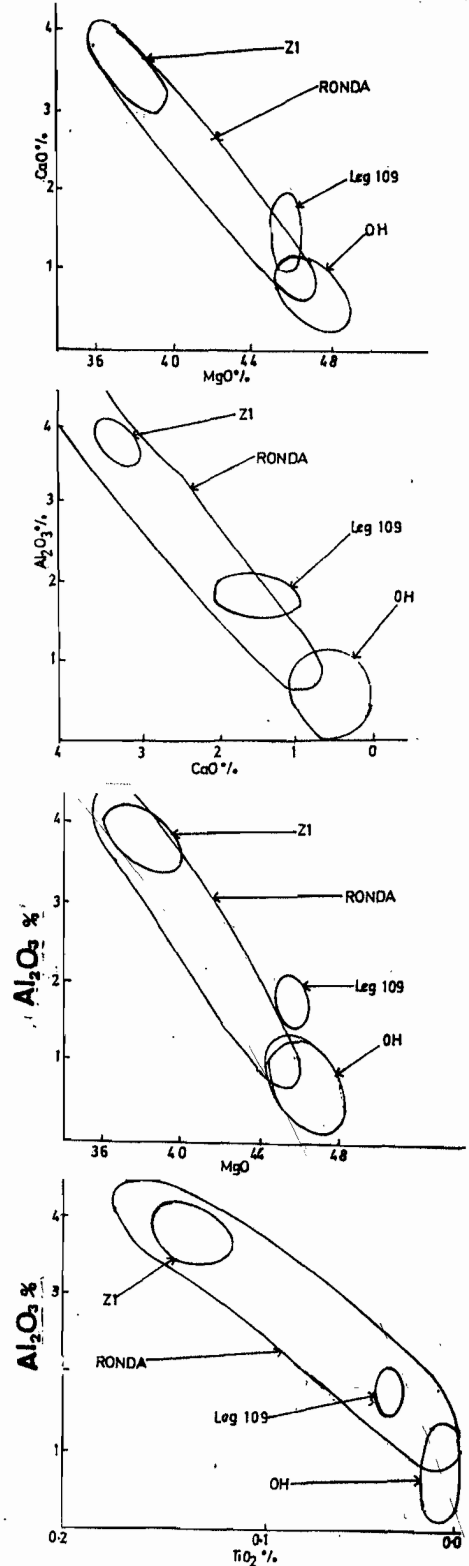


Fig.1: (MgO,CaO), MgO,Al₂O₃), CaO,Al₂O₃), (TiO₂,Al₂O₃) compositions of Leg 109 peridotites. The composition domains of typical mantle peridotitic rocks covering the whole range of residual mantle peridotitic rocks have been drawn for comparison: Ronda orogenic Lherzolites field (Ronda)(Frey et al., 1985), spinel 4herzolites from Zabargad island (ZI)(Bonatti et al., 1986) and the field of highly depleted ophiolitic harzburgites (OH).

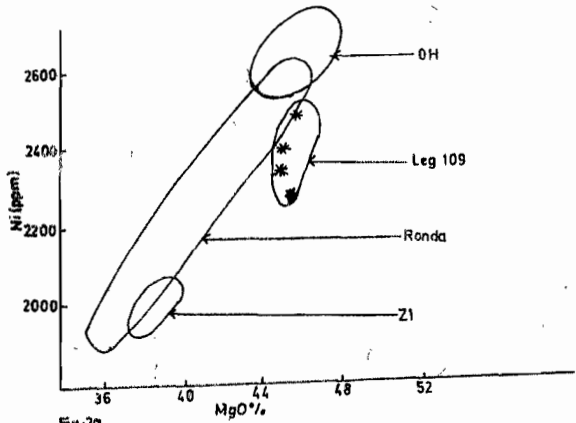


Fig. 2a.

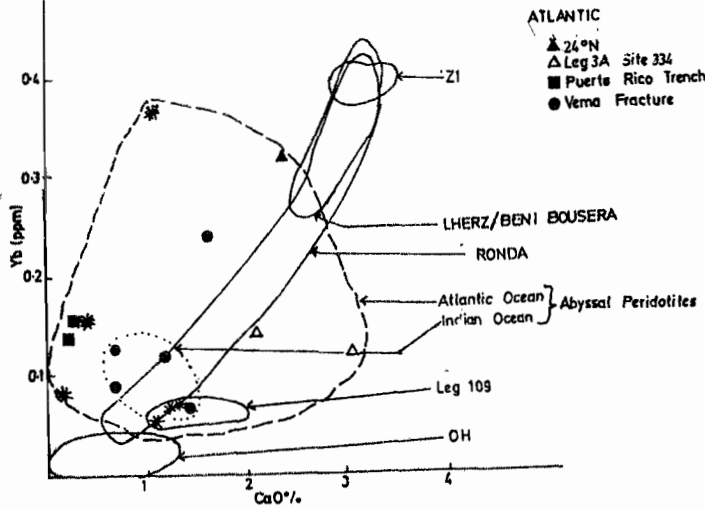


Fig. 2b.

Fig. 2 Trace element compositions of Leg 109 peridotites

Fig. 2a: (MgO, Ni) composition of Leg 109 peridotites. The same mantle peridotite fields as those reported in fig. 1 have been drawn for comparison. (See fig. 1 for comments).

Fig. 2b: (CaO, Yb) composition of Leg 109 peridotites compared with different mantle peridotite types and some abyssal peridotites. The following mantle peridotite fields have been drawn in this diagram: Ronda orogenic peridotite field (Frey et al., 1985), Lherz and Beni Bouchera orogenic peridotite field (Loubet, 1976). Highly depleted ophiolitic harzburgites, Abyssal peridotites from the Indian and Atlantic oceans (Frey, 1985).

are compared again with the compositions of the other classical mantle peridotite types and compared as well in Fig. 2b with some previously studied abyssal rocks (data from Frey, 1985).

REE composition

REE compositions are plotted in the usual chondrite normalized representation (Fig. 3a/b). Some of the samples were unfortunately polished with CeO₂ powder before chemical analysis. This procedure must have affected the elemental composition of Ce and to a lesser extent La. For this reason, the La and Ce contents of four samples were not reported. Three

other samples, which were treated in this same manner, were consequently analyzed in order to obtain the entire REE spectrum. In addition, in two of these additional samples, two different pieces were analyzed. Results of these analyses are shown in fig. 3b. The two pieces analyzed (samples p6-1-5 (30-34) and p9-1-2 (12-14)) are as reported in Fig. 3b. The highly ammonium citrate as a complexing agent (Birck and Allegre, 1978). REE were separated for mass spectrometry in three fractions on a HDEHP (Di(2ethylhexyl) orthophosphoric acid) column (Richard et al., 1976).

serpentinized samples displaying compositions significantly lower than all the other rocks are not taken into account in the analysis of fusion processes.

In comparison with other main types of mantle peridotites (Fig. 4), the Leg 109 peridotites REE patterns are compared with those from other main types of mantle

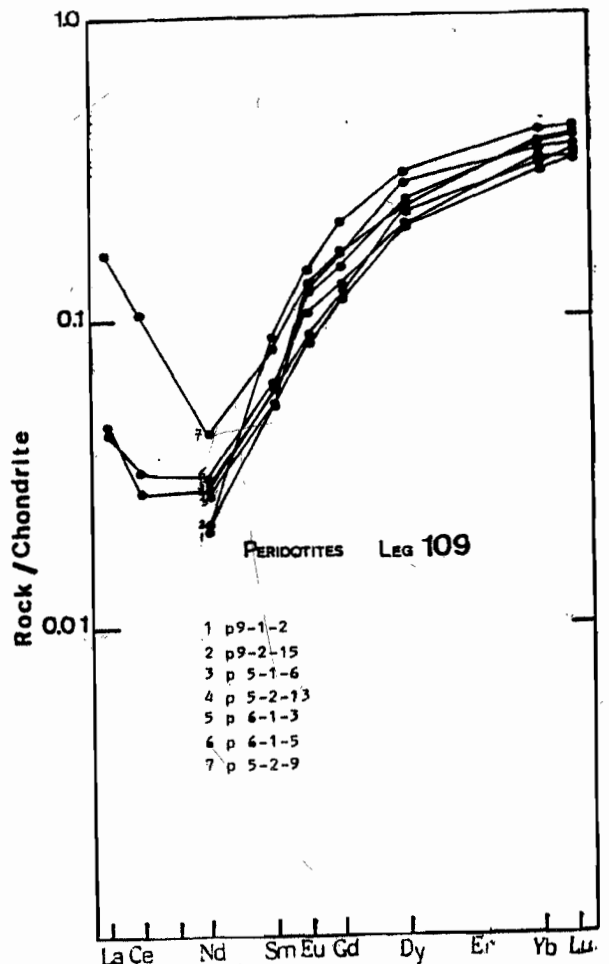


Fig. 3a: REE content of Leg 109 peridotite samples plotted in the classical chondrite normalized representation (the two additional bits analyzed in the samples P9-1-2 and P6-1-5, being excluded)

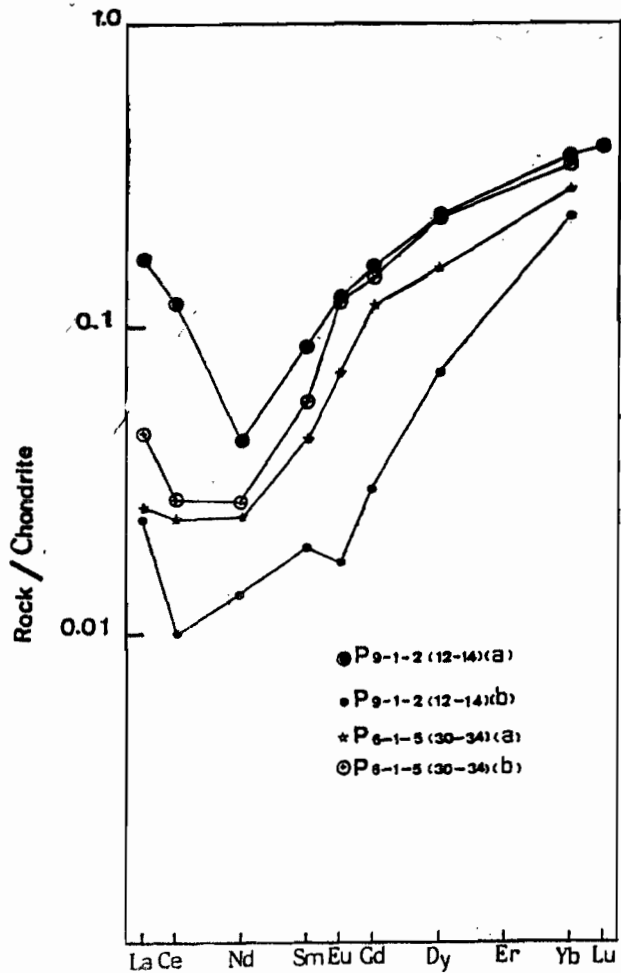


Fig. 3b: REE content of the samples P9-1-2 and P6-1-5 with the additional bits analyzed in each of these samples.

peridotites. Generally, it can also be seen that the REE patterns are intermediate between the slightly depleted orogenic 4herzolites and the highly depleted harzburgites. However, the patterns are very different. Except for sample p6-1-5 (30-34), the REE patterns of all these Leg 109 peridotites are rather similar and are characterized by heavy to intermediate REE contents between 0.3 and 0.5 times that of chondrites and a significant relative depletion of the light REE. A break in the patterns occurs at the Nd with a variable degree of enrichment from Nd to La. This enrichment is slight in samples p6-1-5, but relatively strong in one piece of the p9-1-2 sample.

RESIDUAL MANTLE NATURE OF THE LEG 109 PERIDOTITES

The following modes of origin have been ascribed to abyssal peridotites:

1) Cumulates, from mantle derived magmas. These are known from ophiolitic massifs associated with gabbros and occur

most often at the base of the cumulate series. This type has also been discovered on ocean floor in a few areas such as the Atlantic Ocean (45°N) (Aumento and Loubet, 1971).

(2) Impregnated Peridotites (Peridotites which have interacted with magmas and then recrystallized with a modified composition). These are peridotites found most frequently within the transition zone between the crust and mantle in some ophiolite bodies (Nicolas and Prinzoffer, 1983; Regba and Loubet, 1990).

(3) Residual mantle peridotites. These are classically found in orogenic 4herzolite bodies, in basalt nodules, in ophiolitic massifs. This origin has been assigned also to many abyssal peridotites (Dick and

The geochemical data as well as further criteria support this last origin for these Leg 109 peridotites:

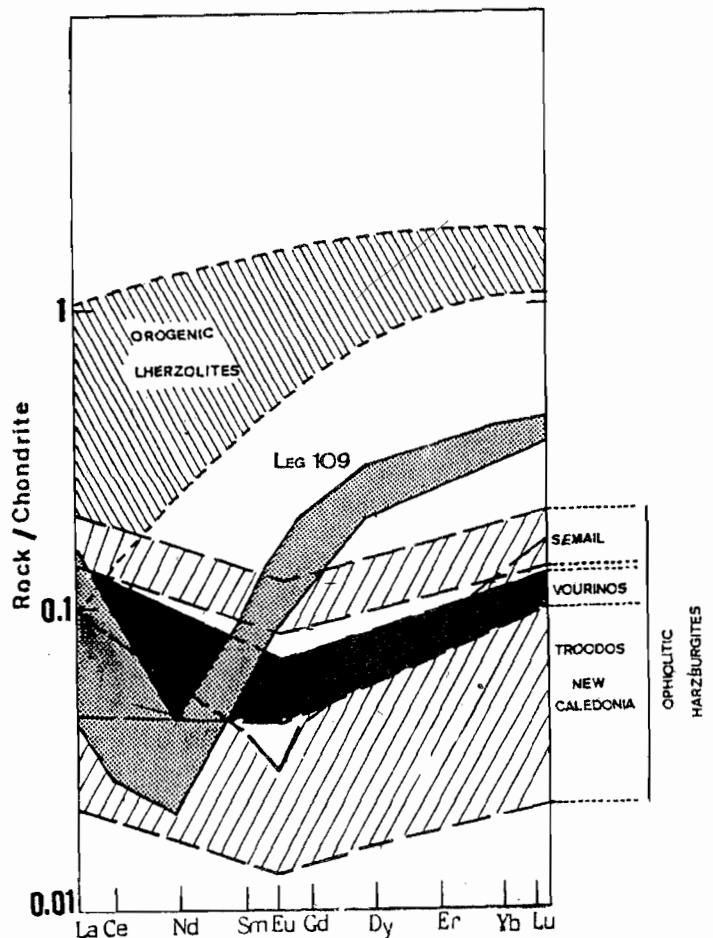


Fig. 4: REE content of Leg 109 peridotite samples compared with the fields of composition of the orogenic 4herzolites and of the ophiolitic harzburgites (the fields of some specific ophiolite bodies have been mentioned). Origin of the data: Orogenic 4herzolites (Loubet et al., 1975; Frey, 1969; Frey et al., 1975; Ottonello et al., 1984 a, b; Ottonello, 1980; Pallister and Knight, 1981; Menzies, 1984).

Major element compositions

In all of the fig.1 diagrams, the leg 109 rocks fall within or close to the main field of the other typical mantle peridotites. The compatibility between the compositions of the Leg 109 peridotite with other mantle peridotite rock is particularly significant when considering diagrams linking two elements, such as Al and Ti (diagram Al_2O_3 , TiO_2) (Fig.1) assumed to be relatively immobile during alteration or serpentinization. Some shifts relative to the field of these mantle peridotites do exist in some diagrams. Further, these small shifts could be attributed to serpentinization effects (MgO enrichment, in particular).

In all of these diagrams the Leg 109 peridotites plot in an intermediate to significantly depleted composition within the field of mantle peridotites. Their MgO, CaO and Al_2O_3 contents indicate that they have relatively marked residual characteristics without attaining the extremely residual characteristics found in harzburgites; MgO = 44 % after correction from serpentinization, Al_2O_3 = 1.5 to 2% (Fig.1).

(2) Minor element composition: Highly significant is the content of some highly compatible trace elements such as Ni, Co or Cr. As a consequence of their high degree of compatibility in magmatic processes, the content of these elements decreases rapidly in the magmas and the solids in a magmatic sequence differentiated through fractional crystallization. The opposite trend is observed in a residual series; Ni and Cr contents increase only slightly in solids as melting progresses. Thus the Ni and Cr composition of these peridotites in the range of other mantle peridotite rocks is indicative of their residual nature (Fig.2)

(3) Mineral composition: Petrological and mineralogical studies of these samples Bullen, (1984), Michael and Bonatti (1985b) for the Atlantic ocean, Dick and Bullen (1984) for the Indian ocean and Bonatti et al. (1986) for the Red Sea (Zabargad).

(Juteau et al., 1990 b; Komor et al., 1990) showed that the chemical composition of the phases, and particularly the unaltered pyroxenes, correspond to rocks equilibrated in the spinel peridotite facies i.e are specific of mantle equilibrated rocks. Spinel compositions also corroborate these conditions of equilibrium: Leg 109 spinel compositions fall in the range of mantle peridotite spinel compositions as defined by Dick and Bullen (1984).

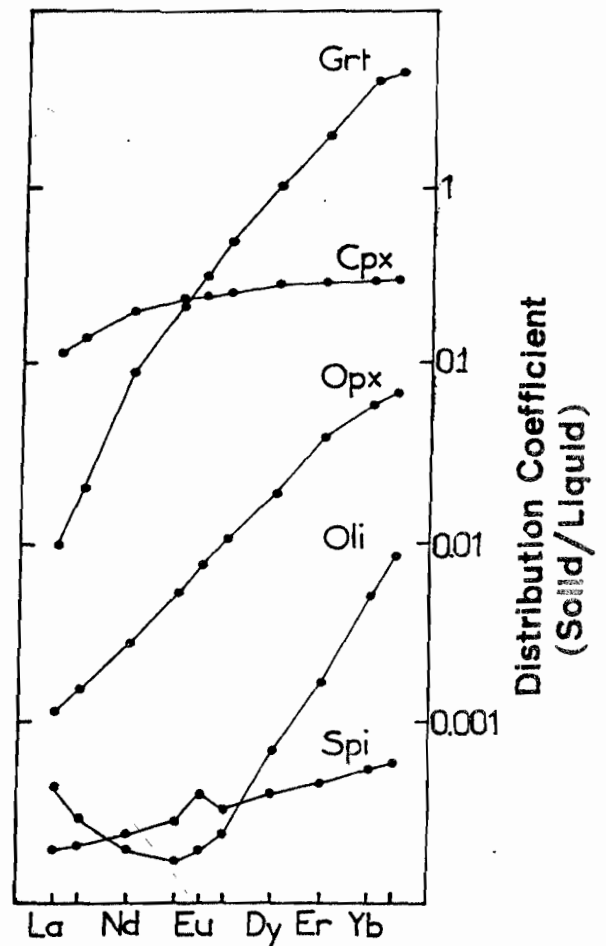


Fig.5: REE partition coefficients used in the models (from Prinzoffler and Allegre, 1985)

(4) Structural characteristics: Tectonic fabric reminiscent of mantle rocks is a characteristic feature of these rocks (Carnat et al., 1990).

(5) As will be shown below, the REE patterns can also fit those of residual peridotites.

ANALYSIS OF FUSION PROCESSES AFFECTING PERIDOTITES FROM LEG 109

In this section, an attempt is made to deduce the fusion conditions of these Mid-Atlantic peridotites from analysis of the REE spectrum. Rare earth elements are well-suited for this type of analysis because their partition coefficients between solid mantle phases and magmas are known (Grutzeck et al., 1974; Irving, 1978; Ottonello, 1980; Stosch, 1982).

For this analysis only the part of the REE spectrum from Nd to heavy REE was taken into account. No consideration was given to the other end of the spectrum (La to Nd) for two reasons, firstly it concerns only a few elements of debatable origin that may not be magmatic or linked to the

serpentinization process, as mentioned previously; secondly, consideration of the Nd to heavy REE section of the spectra is sufficient to constrain the models.

A series of models with different fusion mechanisms was developed (fractional melting, batch melting, disequilibrium melting), to fit the Leg 109 peridotite REE spectra. The models were developed on the basis of the Shaw (1970) equations. The partition coefficients used (fig.5) are identical to those of Prinzoffer and Allegre (1985). Conditions of the

Results of these models applied to peridotites equilibrated successively in the spinel and garnet peridotite facies are presented in fig.6a and fig.6b, respectively.

In each of these figures the models of fractional melting equilibrium, batch melting equilibrium and disequilibrium melting are successively presented.

The results show that two main types of melting mechanism apparently fit the principal characteristics of the REE spectra: (a) the high fractionation from Nd to heavy REE; (b) the relatively low heavy REE content;

(1) **Equilibrium melting processes:** these are processes adequate to induce the high fractionation of Nd compared to the heavy REE, where melting occurs either in the spinel or garnet peridotite facies. Relatively low, heavy REE contents can be obtained when sufficient percentages of partial melting are reached, and for garnet being practically or totally absent at the final stage of melting.

(2) **Disequilibrium melting processes:** in only one case can fusion in disequilibrium produce the intense fractionation of the Nd relative to the heavy REE; this is fusion under spinel peridotite facies in the extreme case where the clinopyroxene has almost completely disappeared (<0.5%) (fig. 6a, disequilibrium melting). In the other cases disequilibrium produces Nd to heavy REE fractionation which is too weak or even reverse (in the case of garnet peridotite facies).

Variations of the partition coefficients would not significantly modify these main conclusions. They depend only on the relative evolution of the REE partition coefficients from light to heavy REE in the main phase which control the distribution of these elements (the clinopyroxene and orthopyroxene phases) and not on the absolute level of these coefficients. At present there is a general agreement among authors as to the relative evolution of the

REE partition coefficients in these two main phases.

The disequilibrium melting process deduced models are specified in the caption of Fig.6.

as theoretically possible on the basis of REE compositions, appears to contradict major element and mineralogical compositions of Leg109 peridotites. The latter composition indicate that the percentage of clinopyroxene remains relatively significant in these rocks. Thin-section observations of the percentage of clinopyroxene before late stage of serpentinization is estimated as approximately 1.5 to 2% (Shipboard Scientific Party, 1988). More critically the present CaO content of these rocks (from 1.0 to 1.9% (water free) permits an evaluation of the clinopyroxene percentage before serpentinization as ranging from 1.5 to 4-5%, from the lower to the highest CaO rich rocks (taking a mean CaO of 20% for Cpx and 4-5% for Opx). When considering high T-P conditions of equilibrium close to those of melt segregation, the higher T-P conditions would favour the formation of solid solutions between more CaO-rich orthopyroxenes and subcalcic clinopyroxenes but the amount of Cpx present in the solid solution would remain significant given the total CaO% of the highest CaO rich rocks.

A few fusion scenarios, which could explain the Leg 109 characteristics, have been retraced in Fig.6c.

The first interesting point to notice in analyzing the results in this figure is that the total melts formed have REE characteristics (the light REE depletion in particular) which can fit those of the basalts from this part of the M.A.R.

The second main point concerns the partial melting processes which are operative: all of these scenarios have at least one stage of equilibrium melting (either fractional or batch melting). In these models, the percentages of melting depend on the mechanisms which operate; fractional melting being more efficient than batch melting in fractionating the REE, the percentages of melting in these scenarios differ according to the role allocated to each of these melting processes. These percentages are relatively low for the model comprising only fractional melting (model D : 4% to 8% fusion for primitive rocks with clinopyroxene percentages varying respectively from 8% to 12%), and higher values are found for the other models (5.5% to 9% for model B : the fractional melting

Fig. 6: Modeling of the partial melting of mantle Ilherzolites in different conditions:

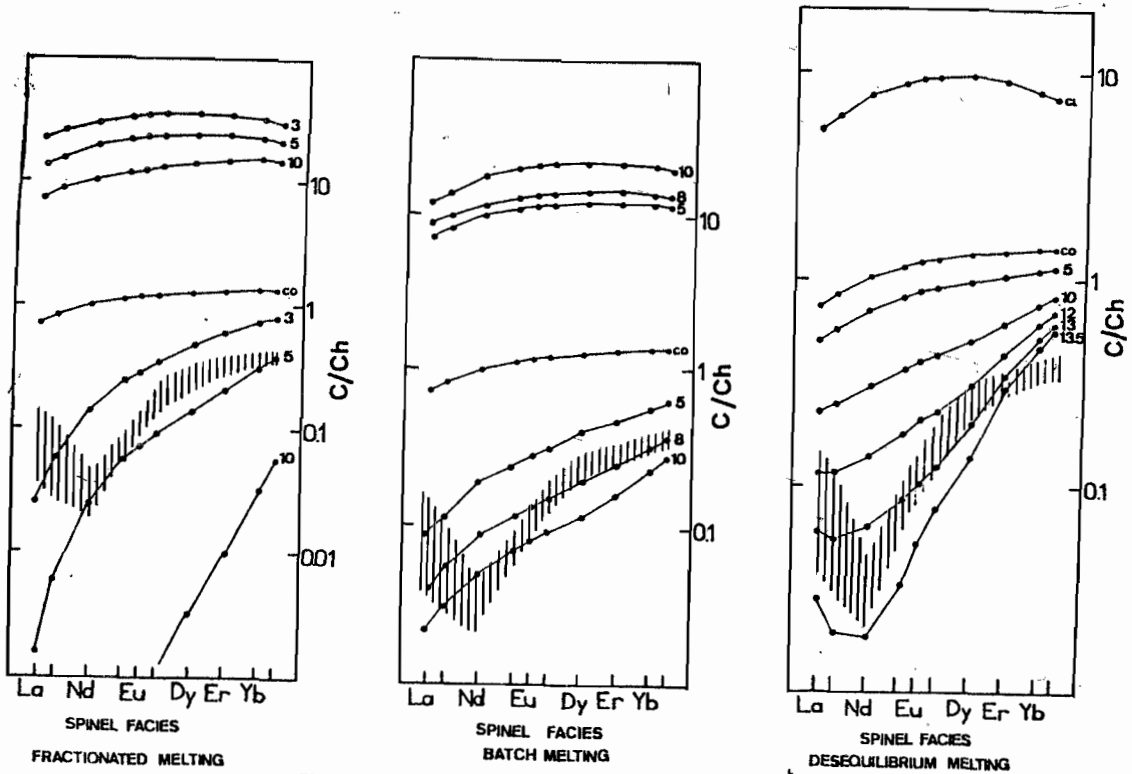


Fig.6a. Successive modeling of fractional, batch and disequilibrium melting processes in the spinel peridotite facies.

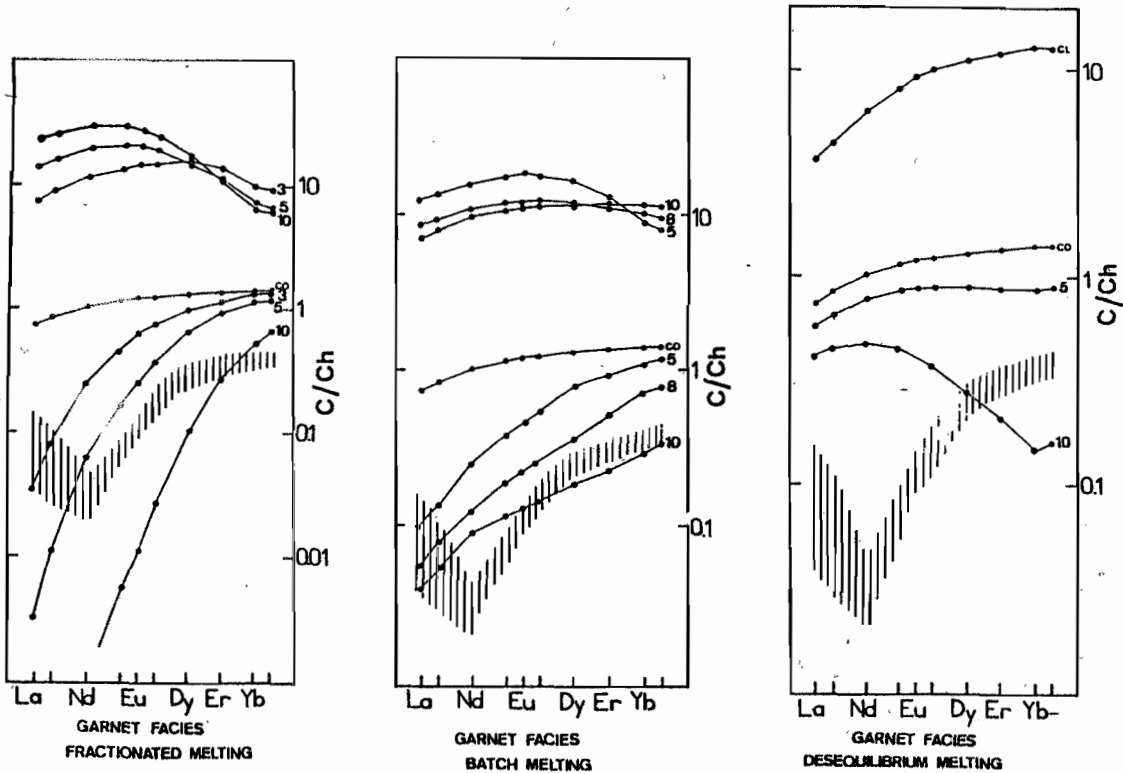


Fig.6b. Successive modeling of fractional, batch and disequilibrium melting processes in the garnet peridotite facies. The REE concentrations of the source (Co), the residual peridotites and the melts produced have been plotted in the chondrite normalized representation (degrees of partial melting mentioned in the respective curves).

Cl: Total liquid in the disequilibrium melting.
 Specified conditions of the models:

	Garnet peridotite		Spinel peridotite	
	Original Proportions	Melting Proportions	Original Proportions	Melting Proportions
OLIV	75	0	75	0
OPX	12	10	15	30
CPX	8	40	8	60
GAR	5	50		
SPI			2	10

Fig.6c: Models of partial melting fitting the Leg 109 REE patterns with the assumed conditions mentioned in the captions of fig.7a and fig.7b.

Successive batch melting processes under different peridotite facies. A first 5% batch melting under the garnet peridotite facies, followed by a second 4% batch melting under spinel peridotite facies.

Successive types of melting under the spinel peridotite facies (or two pyroxene facies which is equivalent from the REE distribution modeling point of view). A first 3% fractional melting, followed by a second 2% batch melting.

Successive types of melting under the spinel peridotite facies. A first 3% fractional melting, followed by a second 8.5% disequilibrium melting.

4% fractional melting under the spinel peridotite facies only.

The REE patterns of the sources (Co), the residual peridotites and the melts produced at different steps as well as the total liquids (Tl) have been plotted. The conditions of each model have been highlighted on each specific curve: successively the facies of the melting peridotite (Spinel or Garnet peridotite facies, denoted Sp or Gt), the type of melting, i.e. either batch, fractional or disequilibrium melting (denoted BM, PM, DM), and the degree of partial melting (denoted by a number).

Independently of the above analysis and based on trace elements, fusion percentages can also be estimated on the basis of major element content (CaO for example) or highly compatible elements, such as Ni. The fusion percentages based on major element analysis are dependent on (1) the chosen initial composition of the rocks, (2) the proportion of minerals considered to have melted. In the same way fusion percentages based on the Ni content also present a measure of uncertainty because of the estimated range of the Ni contents of the initial peridotites (2000 to 2100 ppm), and the range of values measured in the Leg 109 peridotites (2350 to 2490 ppm). Without giving further details on the estimations, the partial melting percentages deduced on this basis are similar to those deduced from REE analysis. Therefore, crude estimations based on the position of the leg 109 peridotites in the general mantle peridotite trend (fig 1 and fig.2) lead to melting proportions ranging from 8 to 15% (assuming as is classically the case that the most highly depleted harzburgites were affected by 20 to 25% partial melting). These percentages look similar to those

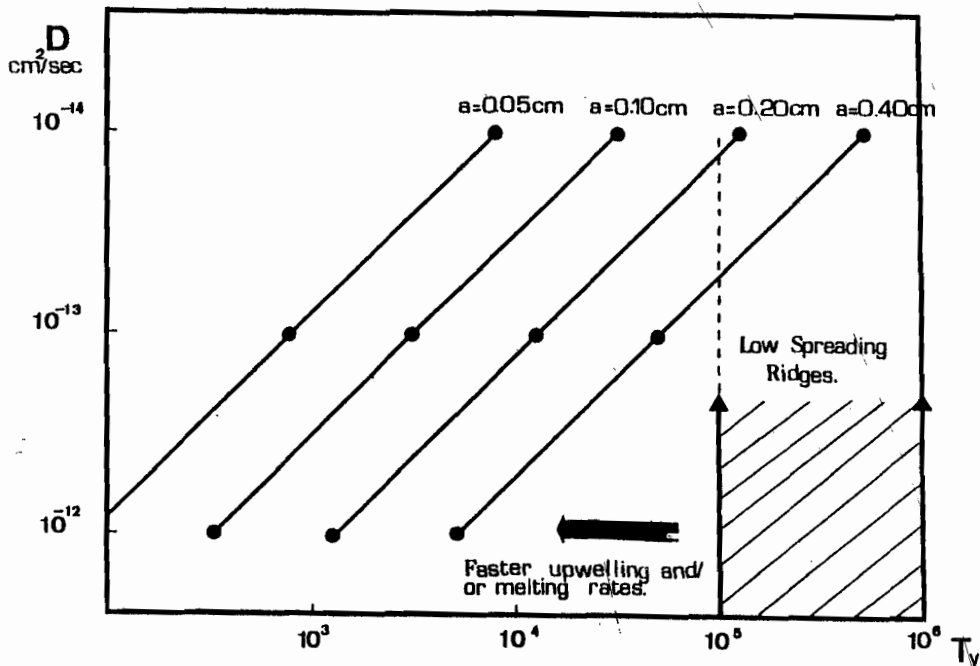


Fig.7 Estimated time of equilibrium between magmas and minerals for different size minerals in function of a range of diffusion coefficients, according to the diffusive time scale equation $t=a^2/D$. (t=time, a=half the size of the mineral in cm, D=diffusion coefficients in cm^2/s)

estimated by Juteau et al., (1990) and Komor et al., (1990) on the basis of mineralogical and whole rock compositions (10% to 15%, and 16% respectively).

These percentages, however, appear to be higher than those from pure fractional melting based models. This type of melting is apparently a physically impossible process because magma extraction requires a certain degree of permeability, the exact level of which is subject to debate

The time required for a mantle diapir to rise from 60 km down (beginning of the fusion zone) to the surface will depend on the mantle upwelling rate. This rate will not necessarily be proportional to the expansion rate of the ocean floor since it will depend on the geometry of the upwelling regime. It and batch melting sequence; 9% to 14% for model A : batch melting under different facies for primitive clinopyroxene percentages varying in the same range).

(McKenzie, 1984).

In summary, the modeling shows:

(1) that the melts produced through the partial melting of Leg 109 peridotite could exhibit REE characteristics of the basalts from this zone; (2) that the partial melting operated at equilibrium either (a) during the entire process (models A, B or D) or (b) at specific stages (model C). The global degree of partial melting depends on the number of batches involved in the process.

It decreases with increasing number of batches (9 to 14% for two batches, 4 to 8% for a large number of batches).

EQUILIBRIUM MELTING IN MANTLE DIAPIRS RISING AT OCEANIC RIDGES

One major conclusion of our modeling concerns the equilibrium melting process assumed to have affected these M.A.R peridotites. A first question concerns the plausibility of this equilibrium melting process to proceed in the conditions of a mantle diapir rising in an oceanic ridge environment. Some quantitative estimations were developed in this respect.

The time necessary for equilibrium to be reached between magmas and crystals of different sizes for a variety of elements will be mainly controlled by the rate of diffusion. In figure 7, classical constraints were chosen to evaluate such time of equilibrium: a mantle peridotite formed by crystals of radius ranging from 0.05 cm to 0.20 cm, diffusion coefficients ranging from 10^{-14} cm²/sec to 10^{-12} cm²/sec (Hoffman and Hart, 1978). The time necessary to reach equilibrium with such

parameters (according to the diffusive time scale $t = a^2/D$) ranges from several hundred years to 10^5 y.

will be equal to the expansion rate of the ocean floor only in the case of symmetry of the upwelling structure relative to a 45° sloping plane, as shown in certain proposed schemes (Bottinga and Allegre (1978).

Taking such a simple upwelling regime as a first approximation for our estimation, the time required for a mantle diapir to rise under such conditions from 60 km depth with expansion rates of 2 cm/year, will be $3.0 \cdot 10^6$ years. Given a degree of partial melting for these rocks of 12%, the time of formation of each batch will depend on the number of batches formed. This time will range from 1.0×10^6 years (4% partial melting in each batch, 3 batches) to 125.000 years (0.5% in each batch, 24 batches). Fig.8 shows that in such conditions, i.e. those of a diapir rising along the axis of a slow spreading ridge, with such a simple, symmetrical upwelling structure, equilibrium can be reached in most cases. Large variations of the chosen parameters would even be acceptable, such as variations of the diffusion coefficients or of the upwelling regime by a factor of ten, for equilibrium to be maintained in most cases. These estimations therefore support the plausibility of the equilibrium in such oceanic environments.

As stressed by McKenzie, (1984), the Th-U disequilibrium evidenced in oceanic basalts is indicative of the occurrence of this equilibrium process. It is also indicative of a low percentage of melting in the batches formed (2% to 0.5%) (McKenzie, (1984). The time of formation of the batches resulting from our estimations is compatible both with the possibility of reaching chemical equilibrium, and with persistency of the Th-U disequilibrium (assuming that the batches of magma are quickly evacuated to the surface after their formation (McKenzie, 1984).

EQUILIBRIUM AND DESEQUILIBRIUM MELTING IN MANTLE PERIDOTITE BODIES

The conclusion of this study concerning the occurrence of an equilibrium type of melting considered to have affected these Leg 109 peridotites disagree with the conclusions of Prinzoffer and Allegre (1985), which explained the V shape of the New Caledonian ophiolitic harzburgites by a series of fusion events under disequilibrium conditions in a rising mantle diapir.

In light of our previous estimations,

these contradictory conclusions can be explained by different conditions of fusion of the bodies. The tendency to form melts in disequilibrium should be increased by higher upwelling rates of the mantle diapirs as well as by larger degrees of partial melting. Therefore for upwelling rates of 10cm/year (corresponding to fast spreading ridge rates of 10cm/year, according to the simplest upwelling regime model) and for degrees of partial melting of the peridotites of 20 to 25% (as in ophiolite bodies), the time of formation of the different batches would range from 125,000 to 12,500 years. The modeling of the fig.7 shows that this time then becomes insufficient to permit equilibrium in some of the cases previously mentioned, but remains sufficient for most others. This may explain the occurrence of both types of processes in the same body, such as is the case apparently in the New Caledonian peridotite (some of the peridotites from this body having characteristics similar to those of the Leg 109 peridotites).

The different mantle peridotite types are explained better now as having been formed in different geodynamic environments (Bonatti and Michael, 1989).

The low percentages of melting of the 4herzolite type bodies are ascribed to emplacement of these bodies in subcontinental environments. Like the abyssal peridotites from trench zones (Bonatti and Michael, 1989), some highly depleted harzburgite type bodies might have evolved in subduction zone environments (some ophiolite bodies display geochemical characteristics in favour of this hypothesis).

The high degree of partial melting of the peridotites would result from the arrival of fluids following the dehydration of the subducted oceanic crust. This addition of water would induce an abrupt decrease of the peridotite solidus. Thus, it seems probable that under such conditions high percentages of melting are reached rather quickly preventing equilibrium to proceed.

Boudier and Nicolas (1986) explained the different characteristics (compositions of the ultramafics, thickness of the crustal section, structures and microstructures) of the major peridotite bodies (orogenic Lherzolite, ophiolitic Harzburgite) as resulting from different rates of the rising mantle diapirs. The conclusions of this analysis are in good agreement with this interpretation and show that the equilibrium/disequilibrium type of melting might represent another interesting

characteristic differentiating the different types of peridotite bodies. However, we

CONCLUSION

Geochemical study of these Leg 109 peridotites from the MAR reveal the following:

- (1) their residual nature;
- (2) the conditions of their partial melting based on their REE data, and shows that this should have operated at equilibrium with moderate degrees of partial melting either during the entire process or at specific stages;
- (3) shows that such characteristics (equilibrated type) are expected when spreading rates and inferred ascent of mantle diapirs are small as at 33°N on the MAR;
- (4) leads to the proposition that the equilibrium/disequilibrium type of melting might represent another interesting characteristic differentiating the mantle peridotite bodies from different geodynamic environments (Lherzolite type bodies, Harzburgite type bodies, this Leg 109 peridotite body), and indicative of their different conditions of melting.

ACKNOWLEDGEMENT:

Peridotite samples from ODP were donated by T. Juteau. The participation of a member of the Laboratoire de Geochimie, Universite Paul Sabatier, Toulouse on the JOIDES resolution was also enabled by him. This work benefited from long discussions with him and E. BERGER as well as from constructive reviews of F. FREY, H. LANGMUIR, G. BREY. We thank the French INSU organization for financial support for the ODP.

REFERENCES -

- Aumento, F., and Loubet, H., 1971. The Mid-Atlantic ridge Near 45°N. Serpentinized ultramafic intrusions. *Can.J. Earth Sci.*, 8/6: 631-663.
- Berger, G., Schott, J. and Loubet, M., 1987. Fundamental Processes controlling the first stage of alteration of a basalt glass by sea water: an experimental study between 200°C and 320°C. *Earth. Planet. Sci. Lett.*, 84: 431-445.

- Birck, J.L., and Allegre, C.J., 1978. Chronology and Chemical history of parent body of basaltic achondrites studied by the $^{87}\text{Rb}/^{87}\text{Sr}$ method. *Earth. Planet. Sci. Lett.* 39: 37-51
- Bonatti, E. Michael, P.J. 1989. Mantle peridotites from continental rifts to ocean basins to subduction zones. *Earth. Planet. Sci. Lett.*, 91: 297-311.
- Bonatti, E., Ottonello, G. and Hamlyn, P.R., 1986. Peridotites from island of Zabargad (St John), Red Sea: petrology and geochemistry. *Journ. Geophys. Res.*, Vol. 91 no. B1: 599-631.
- Bonatti, E., and Hamlyn, P.R., 1981. Oceanic ultramafic rocks, in *The Sea*, vol. 7, *The Oceanic Lithosphere*, 241-283, John Wiley, New York.
- Bottinga, Y., and Allegre, C.J., 1978. Partial melting under spreading ridges. *Phil. Trans. R. Soc. Lond.*, A288: 501-525.
- Boudier, F. and Nicolas, A., 1986. Harzburgite and Lherzolite subtypes in ophiolitic and oceanic environments. *Earth. Planet. Sci. Lett.*, 76: 84-92.
- Bougault, H., Gambon, P., and Toulhouat, H. 1977. X-Ray spectrometric analysis of trace elements in rocks. Correction for instrumental interference. *X Ray Spectrometry*, 6: 66- 72.
- Cannat, M., Juteau, T., and Berger, E., 1990. In Detrick, R., Honnorez, J., Bryan, W.B., 1990. *Proc. ODP. Init. Repts.*, 106/109: College Station, TX (Ocean Drilling Program), 47-56.
- Dick, H.J.B., and Bullen, T. 1984. Chromium spinel as a petrogenetic indicator in abyssal and alpine-type peridotites and spatially associated lava. *Contrib. Miner. Petrol.*, 86: 54-76.
- Dick, H.J.B., Fisher, R.L., and Bryan W.B., 1984. Mineralogical variability in the uppermost mantle along Mid-Ocean Ridges. *Earth. Planet. Sci. Lett.*, 69: 88-106.
- Frey, F.A., 1969. Rare earth abundance in a high-temperature peridotite intrusion. *Geochim. Cosmochim. Acta*, 33: 1429-1447.
- Frey, F.A. 1982. Rare earth element in Upper mantle rocks. In *Rare Earth Elements Geochemistry*, P. Henderson, ed., 153-204, Elsevier.
- Frey, F.A. Suen, C.J. and Stuckman H.W., 1985. The Ronda high temperature peridotite: geochemistry and petrogenesis. *Geochim. Cosmochim. Acta*, 49: 2469-2491.
- Grutzeck, S.J. Kridelbaugh, and Weill, D.F., 1974. The distribution of Sr and the REE between diopside and silicate liquid. *Geophys. Res. Lett.*, 1: 273.
- Hofmann, A.W. and Hart, S.R., 1978. An assessment of local and regional isotopic equilibrium in the mantle. *Earth. Planet. Sci. Lett.*, 38: 44.
- Irving, A.J., 1978. A review of experimental studies of crystal/liquid trace element partitioning. *Geochim. Cosmochim. Acta*, 42: 743.
- Juteau, T., Berger, E., Cannat, M., 1990. In Detrick, R., Honnorez, J., Bryan, W.B., 1990. *Proc. ODP. Init. Repts.*, 106/109: College Station, TX (Ocean Drilling Program), 27-44.
- Juteau, T., Cannat, M., and Lagabrielle Y., 1990. In Detrick, R., Honnorez, J., Bryan, W.B., 1990. *Proc. ODP. Init. Repts.*, 106/109: College Station, TX (Ocean Drilling Program), 303-308.
- Karson, J.A., Thompson, G., and Humphris, S.E., 1987. Along axis variations in sea floor spreading in the MARK area. *Nature*. 328: 681-685.
- Komor, S.C., Grove, T.L., and Hebert, R., 1990. In Detrick, R., Honnorez, J., Bryan, W.B., 1990. *Proc. ODP. Init. Repts.*, 106/109: College Station, TX (Ocean Drilling Program), 85-101

- Lar, U.A. 1991 Etude Geochimique de massif mafic/Ultramafic (Apa, Todasana, Tinaquillo) de la chaîne Tertiaire Caraïbe du Venezuela: Genèse de magma mantellique et interaction manteau-croûte. unpublished Ph.D Thesis, UPS Toulouse, France.
- Loubet, M., 1976. Geochimie des Terres Rares dans les massifs de peridotites dits de haute température: évolution du manteau terrestre. Unpublished Thesis, Univ Paris 7..
- Loubet, M., Shimizu, N. and Allegre, C.J., 1975. Rare earth elements in Alpine peridotites. *Contrib. Mineral. Petrol.*, 53:1
- McKenzie, D., 1984. The generation and compaction of partially molten rocks. *J. Petrology*, 25: 713-765.
- Menzies M., 1984. Chemical and isotopic heterogeneity in orogenic and ophiolitic peridotites. In "Ophiolites and Oceanic lithosphere" (eds. I. G. Gass, S. J. Lippard and A.W. Shelton), 231-240, Blackwell scientific.
- Michael, P.J. and Bonatti, E. 1985a. Petrology of ultramafic rocks from sites 556, 558 and 560 in the North Atlantic. Initial Report D.S.D.P., vol. 82: 523-530
- Michael, P.J. and Bonatti E., 1985b. Peridotite composition in the North Atlantic: regional and tectonic variations and implications for partial melting. *Earth. Planet. Sci. Lett.*, 73: 91-104.
- Michard, A., Albaredo, F., Michard, G., Minster, J.F. and Charlou, J.L., 1983. Rare-earth elements and Uranium in high temperature solutions from East Pacific Rise hydrothermal vent field (13°N). *Nature*, 303: 795-797.
- Michard, A., Beaucaire, C., and Michard, G., 1987. Uranium and Rare earth elements in CO₂-rich waters from Vals-les Bains (France). *Geoch. Cosmoch. Acta.*, 51: 901-909.
- Nicolas, A., 1986. A melt extraction model based on structural studies in mantle peridotites. *Journal of Petrol.*, Vol.27., 4: 999-1022.
- Nicolas, A., and Jackson, E.D., 1972. Repartition en deux provinces des peridotites des chaînes alpines longeant la Méditerranée: implications géotectoniques. *Schweiz. Mineral. Petrogr. Mitt.*, 52: 479-495.
- Nicolas, A. and Prinzoffer, A., 1983. Cumulative or residual origin for the transition zone in ophiolites: structural evidence. *J. Petrol.* 24: 188-206
- Ottonello, G., 1980. Rare earth abundance and distributions in some spinel peridotite xenoliths from Assab (Ethiopia). *Geochim. Cosmochim. Acta.* 44: 1885
- Ottonello, G., and Ernst, W.G., 1979. Petrogenesis of some Ligurian peridotites, II rare earth element chemistry. *Geochim. Cosmochim. Acta*, 43, 1273-1284.
- Ottonello, G., Ernst, W.G., and Joron, J.L., 1984a. Rare earth and 3d transition element geochemistry of peridotitic rocks: I. Peridotites from the Western Alps. *J. Petrol.*, 25: 343-372.
- Ottonello, G., Joron, J.L., and Piccardo, G.B., 1984b. Rare earth and 3rd transition element geochemistry of peridotitic rocks: II Ligurian peridotites and associated basalts., *J. Petrol.*, 25: 343-372.
- Pallister, J.S., and Knight, R.J., 1981. Rare earth element geochemistry of the Semail ophiolite near Ibra, Oman. *J. Geophys. Res.*, 86: 2673.
- Prinzoffer, A. and Allegre, C.J., 1985. Residual peridotites and the mechanisms of partial melting. *Earth, Planet. Sci. Lett.* 74: 251-265.
- Regba, M. and Loubet, M. Impregnated peridotite in the transition zone of the Haylayn block of the Oman ophiolite. In preparation.

- Richard, P., Shimizu, N., and Allegre, C.J., 1976. $^{143}\text{Nd}/^{144}\text{Nd}$ a natural tracer: an application to oceanic basalts. *Earth. Planet. Sci. Lett.*, 31: 169-178.
- Shaw, D.M., 1970. Trace element fractionation during anatexis. *Geochim. Cosmochim. Acta*, 34: 237.
- Shin, C.Y. 1972. The rare earth geochemistry of oceanic igneous rocks. Ph.D Thesis, Columbia Univ., New York.
- Shipboard Scientific Party, 1988. Site 670, in Bryan, W.B., Juteau, T., et al., *Proc. ODP. Init. Repts. (Pt A)*. 109: College Station, TX (Ocean Drilling Program) 202-227.
- Spera, F.J., 1980. Aspect of magma transport. In Hargraves, R.B.(ed.) *Physics of magmatic processes*. Princeton Univ. Press.: 265-323.
- Stiosch, H.G., 1982. Rare earth element partitioning between minerals from anhydrous spinel peridotite xenoliths. *Geochim. Cosmochim. Acta*, 46: 793.
- Suen, C.J., Frey, F.A., and Malpas, J., 1979. Bay of Islands ophiolite suite, Newfoundland: petrologic and geochemical characteristics with emphasis on rare earth element geochemistry. *Earth. Planet. Sci. Lett.*, 45: 337-348.